Assimilating in situ and radar altimetry data into a large-scale hydrologic-hydrodynamic model for streamflow forecast in the Amazon

R. C. D. Paiva, W. Collischonn, Marie-Paule Bonnet, L. G. G. de Goncalves, S. Calmant, A. Getirana, J. S. da Silva

Hydrol. Earth Syst. Sci. Discuss., 10, 2879–2925, 2013
www.hydrol-earth-syst-sci-discuss.net/10/2879/2013/
doi:10.5194/hessd-10-2879-2013

Hydrology and Earth System Sciences
Discussions

Assimilating in situ and radar altimetry data into a large-scale hydrologic-hydrodynamic model for streamflow forecast in the Amazon

R. C. D. Paiva[1,2], W. Collischonn[1], M.-P. Bonnet[2], L. G. G. de Gonçalves[3], S. Calmant[4], A. Getirana[5], and J. Santos da Silva[6]

[1]Instituto de Pesquisas Hidráulicas IPH, Universidade Federal do Rio Grande do Sul UFRGS, Porto Alegre, Brazil
[2]Géosciences Environnement Toulouse GET, UMR5563, CNRS IRD UPS, OMP, Université Toulouse III Paul Sabatier, Toulouse, France
[3]CPTEC/INPE – Centro de Previsão de Tempo e Estudos Climáticos, Instituto Nacional de Pesquisas Espaciais, Cachoeira Paulista, Brazil
[4]Laboratoire d'Etudes en Géophysique et Océanographie Spatiales LEGOS, UMR5566, CNES CNRS IRD UPS, OMP, Université Toulouse III Paul Sabatier, Toulouse, France
[5]NASA Goddard Space Flight Center, Hydrological Sciences Lab, Greenbelt, USA
[6]Universidade do Estado do Amazonas UEA, Manaus, Amazonas, Brazil

Received: 1 February 2013 – Accepted: 26 February 2013 – Published: 7 March 2013

Correspondence to: R. C. D. Paiva (rodrigocdpaiva@gmail.com)

Published by Copernicus Publications on behalf of the European Geosciences Union.

Abstract

In this work we introduce and evaluate a data assimilation framework for gauged and radar altimetry-based discharge and water levels applied to a large scale hydrologic-hydrodynamic model for stream flow forecasts over the Amazon River basin. We used the process-based hydrological model called MGB-IPH coupled with a river hydrodynamic module using a storage model for floodplains. The Ensemble Kalman Filter technique was used to assimilate information from hundreds of gauging and altimetry stations based on ENVISAT satellite data. Model state variables errors were generated by corrupting precipitation forcing, considering log-normally distributed, time and spatially correlated errors. The EnKF performed well when assimilating in situ discharge, by improving model estimates at the assimilation sites and also transferring information to ungauged rivers reaches. Altimetry data assimilation improves results at a daily basis in terms of water levels and discharges with minor degree, even though radar altimetry data has a low temporal resolution. Sensitivity tests highlighted the importance of the magnitude of the precipitation errors and that of their spatial correlation, while temporal correlation showed to be dispensable. The deterioration of model performance at some unmonitored reaches indicates the need for proper characterization of model errors and spatial localization techniques for hydrological applications. Finally, we evaluated stream flow forecasts for the Amazon basin based on initial conditions produced by the data assimilation scheme and using the ensemble stream flow prediction approach where the model is forced by past meteorological forcings. The resulting forecasts agreed well with the observations and maintained meaningful skill at large rivers even for long lead times, e.g. >90 days at the Solimões/Amazon main stem. Results encourage the potential of hydrological forecasts at large rivers and/or poorly monitored regions by combining models and remote sensing information.

1 Introduction

Land surface waters play an important role in global water cycle and earth system, regulating freshwater discharge from land into oceans (Oki and Kanae, 2006) and also land-atmosphere exchanges of water, energy (Krinner, 2003; Decharme et al., 2012) and gases such as methane (Gedney et al., 2004). Moreover, it affects directly society that uses it for drinking water and also transportation of people and goods, agriculture and energy production from hydropower. More specific to the Amazon basin, important extreme hydrological events have occurred recently, for instance, the 2009 and 2012 floods and the 1996, 2005 and 2010 droughts (Chen et al., 2010; Tomasella et al. 2010; Marengo et al., 2008; Espinoza et al., 2011; Marengo et al., 2011). These events caused several impacts on local population that strongly depends on the rivers and is very vulnerable to floods since most settlements lie along the rivers.

In situ measurements of river stage and discharge at stream gauges are the most conventional alternative for monitoring surface waters, although observation networks are rather sparse at several regions such as the Amazon River basin. Alternatively, radar altimetry techniques have been developed in past years to monitor water levels (e.g. Santos da Silva et al., 2010; Alsdorf et al., 2007) or discharges using rating curves (e.g. Leon et al., 2006; Papa et al., 2010a; Getirana and Peters-Lidard, 2013). If compared to in situ gauges in remote regions, these satellite instruments can provide observations with much better spatial resolution, but with worse temporal sampling. Moreover, the forthcoming Surface Water and Ocean Topography (SWOT) mission (Durand et al., 2010a) is designed to provide high resolution images of inland water surface elevation, including rivers, lakes, wetlands and reservoirs, using a swath mapping radar altimeter with high frequency repeat orbit. Additionally, it may also be possible to derive discharge estimates from SWOT data by using specially developed algorithms (e.g. Durand et al., 2010b).

In contrast, there are several efforts on hydrological modeling to simulate processes as river and floodplain dynamics in large river basins such as the Amazon (Paiva et al.,

Discussion Paper | Discussion Paper | Discussion Paper | Discussion Paper |

2012, 2013; Yamazaki et al., 2011; Getirana et al., 2012; Decharme et al., 2012; Coe et al., 2008; Wilson et al., 2007; Trigg et al., 2009). These models can potentially provide detailed information on surface waters, both spatially and temporally, but such estimates are somehow imperfect due to uncertainty in model structure, parameters and forcing data (Liu and Gupta, 2007).

Data assimilation (DA) methods are an alternative to optimally merge uncertain model predictions with both in situ and the newly remote sensing observations of surface waters. The aim of DA techniques is to "produce physically consistent representations or estimates of the dynamical behaviour of a system by merging the information present in imperfect models and uncertain data in an optimal way to achieve uncertainty quantification and reduction" (Liu and Gupta, 2007). Such methods can also be used to estimate balanced initial states of hydrological models for forecasting the aforementioned extreme events. There are already some hydrological regional/global forecast systems founded on physically-based hydrological models (e.g. Wood et al., 2002; Thielen et al., 2009; Alfieri et al., 2012), and also several physical modeling experiments in the Amazon basin, as previously mentioned. However, current attempts for developing hydrological forecasts in this basin are mostly based on statistical methods (e.g. Uvo and Grahan, 1998; Uvo et al., 2000). Furthermore, Paiva et al. (2012b) showed that, for lead times up to 3 months, uncertainty of initial conditions plays a major role for discharge predictability on main Amazonian Rivers, if compared to the importance of precipitation forcing, suggesting the importance of DA techniques for streamflow forecasts in this region.

Research on data assimilation applied to hydrology has increased in past years with various applications utilizing Kalman filters (e.g. the Ensemble Kalman Filter – EnKF, developed by Evensen, 2003), particle filters or variational methods, as extensively reviewed in Liu and Gupta (2007), Reichle (2008) and Liu et al. (2012). These applications include a wide range of observations, both in situ and remotely sensed, data assimilation methods and models representing different hydrological processes, at different spatial scales and with several objectives, such as: the assimilation of snow

(Andreadis and Lettenmaier, 2006) and soil moisture (Reichle et al., 2002) data into land surface models using the EnKF; assimilation of in situ water level measurements into a small scale 1-D hydrodynamic model for flood forecast using Kalman filtering methods (Neal et al., 2007; Ricci et al., 2011); assimilation of synthetic SWOT data into hydrodynamic models at restricted areas using the EnKF and some variations (Biancamaria et al., 2011; Andreadis et al., 2007; Durand et al., 2008); assimilation of discharge data into distributed hydrological models (Clark et al., 2008; McMillan et al., 2013; Lee et al., 2012; Thirel et al., 2010; Rakovec et al., 2012) using the EnKF or variational methods; simultaneous assimilation of soil moisture and discharge data into a distributed hydrological model using variational DA (Lee et al., 2011); assimilation of radar altimetry data of reservoir water levels using the EnKF (Pereira-Cardenal et al., 2011); development of a modelling platform (Land Information System – LIS) to merge multiple in situ and remotely sensed observations with land surface models (Kumar et al., 2008); merging water levels information derived from a satellite Synthetic Aperture Radar (SAR) image and digital terrain model (DTM) with a 1-D hydrodynamic model for estimating river discharge (Neal et al., 2009); among others. Although there is an extensive bibliography on hydrological data assimilation, the current state of the art regional/global hydrological prediction systems (e.g. Thielen et al., 2009; Alfieri et al., 2012) still do not incorporate advanced data assimilation systems for updating model initial states. Also, the assimilation of discharge and water levels from in situ and remotely sensed observations into regional/global hydrologic-hydrodynamic models is still uncommon.

In this paper, we present the development and evaluation of a data assimilation framework for both gauged and radar altimetry-based discharge and water levels into a large scale hydrologic-hydrodynamic model of the Amazon River basin using the EnKF. We also explore the usefulness of such system to provide streamflow forecasts when forced by past remotely sensed precipitation data and based mostly on model initial conditions. This paper is in the context of recent developments of techniques for integrating information from hydrological models with newly remotely sensed data such as the forthcoming SWOT mission and also in the context of regional/global hydrological forecast systems including large, poorly gauged river basins. Through our experimental results, we explore questions such as: is an EnKF-based DA scheme feasible for assimilating discharge and water level data into large scale hydrologic-hydrodynamic models? Is it able to improve discharge and water level estimates at sites where data were assimilated and also at ungauged rivers? Does the assimilation of radar altimetry data also improve model estimates at large river basins, considering that it has lower temporal resolution and accuracy if compared to gauged in situ data? Would it be possible to provide accurate streamflow forecasts at large basins such as the Amazon using a large scale hydrologic-hydrodynamic model based mostly on the initial hydrological states gathered by the DA scheme? At which spatial and temporal scales?

2 Methods

2.1 The hydrologic-hydrodynamic model

We used the MGB-IPH model (Collischonn et al., 2007), which is a large scale, distributed and process-based hydrological model with a hydrodynamic module described in Paiva et al. (2011). It simulates surface energy and water balance and also discharge, water level and flood inundation on a complex river network. Vertical hydrological processes include soil water budget using a bucket model, energy budget and evapotranspiration using the Penman Monteith approach, and also surface, subsurface and groundwater flow generation, among others. The flow generated within each catchment is routed to the stream network using a linear reservoir type model. River flow routing is performed using a combination of either a Muskingum-Cunge (MC) method or a hydrodynamic model (HD).

The hydrodynamic model of MGB-IPH (Paiva et al., 2011) solves the full 1-D Saint-Venant equations for the river network and flood inundation is simulated using a simple

model assuming that the floodplains act only as storage areas. River-floodplain parameters (river width, bottom levels, roughness coefficient, floodplain bathymetry) are estimated using GIS-based algorithms from the Shuttle Radar Topography Mission (SRTM) Digital Elevation Model (DEM) (Farr et al., 2007) and using geomorphological relations.

2.2 The Ensemble Kalman Filter

The goal of data assimilation is to combine the uncertain and complementary information from measurements and simulation models into an optimal estimate of the hydrological fields of interest, providing a general framework for dealing with uncertainty from measurements and also input, output and model structure (Reichle, 2008; Liu and Gupta, 2007; Liu et al. 2012; Vrugt et al., 2005).

A great part of the hydrological applications of data assimilation methods uses schemes based on the Kalman filter (Kalman, 1960), specially the Ensemble Kalman Filter (Evensen, 2003, 2009), which is also used in this study and is briefly described below. The model representing the dynamics of the simulated system can be represented in a discrete form by the process equation:

$$\boldsymbol{x}_{k+1} = M(\boldsymbol{x}_k, \boldsymbol{u}_k, \boldsymbol{\theta}) + \boldsymbol{q}_k \tag{1}$$

where $\boldsymbol{x}$ represents the state variables and, $\boldsymbol{u}$ and $\boldsymbol{\theta}$ represent model forcings and parameters, respectively, M is the nonlinear model operator that relates model states from time interval t_k to $t_{k+1} = t_k + \Delta t$, and $\boldsymbol{q}_k$ represents errors in model structure, parameter, forcings and antecedent states. In this study, $\boldsymbol{x}$ is a vector composed by all MGB-IPH state variables, i.e. soil moisture, storage and discharge from surface, subsurface and groundwater reservoirs, soil temperature, canopy storage and river discharge and water level. The measurement equation is defined by:

$$\boldsymbol{y}_k = H(\boldsymbol{x}_k) + \boldsymbol{\varepsilon}_k \tag{2}$$

where $\boldsymbol{y}$ is observation vector, $\boldsymbol{\varepsilon}$ is the vector of observation errors and H is the observation operator which relates the model state variables vector $\boldsymbol{x}$ to the observations vector $\boldsymbol{y}$. In our case, observations are river discharges or water levels at selected sites.

In the context of forecast systems and sequential data assimilation methods, at each time interval, the model is integrated in time using Eq. (1) to provide a short-term forecast (or background) $\boldsymbol{x}^f_{k+1}$ and whenever an observation is available, the forecast errors are computed as $(\boldsymbol{y}_{k+1} - H(\boldsymbol{x}^f_{k+1}))$. Therefore, the goal of data assimilation is to obtain an optimal estimate of model state variables $\boldsymbol{x}^a$ (called analysis) given model and observation errors. In the case of the original Kalman Filter (Kalman, 1960), the DA problem is solved using a linear estimator assuming that (i) model and observation operators (M and H) are linear; (ii) observation errors are unbiased and both temporally and spatially uncorrelated; (iii) model errors are unbiased and temporally uncorrelated; and (iv) there is no correlation between model and observation errors. Consequently, an unbiased and minimum variance estimate of model states is obtained by:

$$\boldsymbol{x}^a = \boldsymbol{x}^f + \mathbf{K}\left(\boldsymbol{y} - \mathbf{H}\boldsymbol{x}^f\right) \tag{3}$$

$$\mathbf{K} = \mathbf{P}^f\mathbf{H}^T\left(\mathbf{H}\mathbf{P}^f\mathbf{H}^T + \mathbf{R}\right)^{-1} \tag{4}$$

where $\mathbf{K}$ is the Kalman gain, $\mathbf{P}$ is the covariance of model errors $\boldsymbol{q}$, and $\mathbf{R}$ is the covariance of measurement errors $\boldsymbol{\varepsilon}$. The Kalman filter also provides the maximum likelihood solution of the DA problem when model and measurement errors are assumed to be also Gaussian. However, the applicability of the KF is limited since most hydrological systems exhibit nonlinear dynamics (Liu and Gupta, 2007) and the assumptions about model errors (e.g. Gaussian, unbiased, among others) are not always valid. Moreover, both the original KF and also its non-linear version, the Extended KF (EKF), have additional drawbacks when applied in large and complex systems with lots of state variables (e.g. distributed hydrological models) due to extra programming and heavy computational requirements associated with the storage and forward integration of the error covariance matrix $\mathbf{P}$ (Vrugt et al., 2005).

Evensen (2003) presented the Ensemble Kalman Filter (EnKF), which is a stochastic or Monte Carlo alternative for the deterministic EKF (Evensen, 2009). In this method, observations and model states are perturbed using a priori-known errors and by means of the model operator M, the algorithm generates an ensemble of model trajectories from which the time evolution of model errors and error covariance matrix can be sampled:

$$\mathbf{P}^f \cong \mathbf{P}^f_e = \overline{\left(\boldsymbol{x}^f - \overline{\boldsymbol{x}^f}\right)\left(\boldsymbol{x}^f - \overline{\boldsymbol{x}^f}\right)^T}, \quad \mathbf{P}^a \cong \mathbf{P}^a_e = \overline{\left(\boldsymbol{x}^a - \overline{\boldsymbol{x}^a}\right)\left(\boldsymbol{x}^a - \overline{\boldsymbol{x}^a}\right)^T} \tag{5}$$

Each ensemble member is then updated using the same analysis equation from the original KF (Eqs. 3 and 4). Alternatively, efficient computational implementations of the EnKF are presented in Evensen (2003, 2004 and 2009) (see http://enkf.nersc.no/ for Fortran codes) where the explicit computation and storage of $\mathbf{P}$ are not required. We used the square root scheme presented in Evensen (2004, 2009) where the perturbation of measurements is not performed, in order to reduce sampling errors.

For linear systems and with large ensemble sizes, the EnKF provides the same solution as the KF method. However, it is noteworthy that it does not fully take into account non-Gaussian errors nor solve the Bayesian update equation for non-Gaussian probability distribution functions. Still, it is a computational efficient analysis scheme for nonlinear models that provides a satisfactory solution, although it is suboptimal, that somehow lies between a linear Gaussian update and a full Bayesian computation (Evensen, 2009).

2.3 Uncertainty in precipitation forcing

We perturbed model states variables by adding a noise in precipitation forcing, considering (i) that this is the most uncertain model input (Liu et al., 2012) and possibly the most important source of model uncertainty and (ii) that this is a proper method to generate physically coherent model errors. A similar approach performed satisfactorily in other hydrological applications of DA methods such as Andreadis and Lettenmaier

Discussion Paper | Discussion Paper | Discussion Paper | Discussion Paper |

(2006) and Biancamaria et al. (2011). Precipitation values were corrupted using a log-normally distribution as presented by Nijjsen and Lettenmaier (2004) and also applied by Andreadis and Lettenmaier (2006):

$$P_c = \frac{1+\beta}{\sqrt{E^2+1}} \exp\left(\sqrt{\ln\left(E^2+1\right)}\, s\right) P \tag{6}$$

where P_c (mm Δt^{-1}) is the perturbed daily precipitation, P (mm Δt^{-1}) is the unperturbed daily precipitation, E is the relative error (%), β is the relative bias and $s \sim N(0,1)$ is a normally distributed and spatially correlated random variable with zero mean and unit variance. Spatially correlated pseudo random fields $\boldsymbol{w}$ were generated by means of the algorithm based on the two dimensional Fourier transform presented in Evensen (2003) (see http://enkf.nersc.no/ for Fortran codes), having zero mean, unit variance and isotropic covariance function decreasing to the e^{-1} value at the distance τ_x called spatial decorrelation length. At each spatial location, temporal correlation was also considered using the following equation for simulating the time evolution of errors (Evensen, 2003):

$$s_k = \alpha s_{k-1} + \sqrt{1-\alpha^2}\, w_{k-1} \tag{7}$$

where k is the time interval, s_k is a sequence of time correlated errors with zero mean and unit variance (input for Eq. 6) and α determines the time decorrelation of the stochastic forcing, e.g. $\alpha = 0$ generates a sequence of white noise while $\alpha = 1$ removes the stochastic forcing. The parameter α is determined by:

$$\alpha = 1 - \frac{\Delta t}{\tau_t} \tag{8}$$

where τ_t is the temporal decorrelation length, that determines that s decreases by the ratio e^{-1} after a time period $t = \tau_t$ if the stochastic term w is excluded.

2.4 Measurement errors

Water level (z) and discharge (Q) observations errors were modeled using the following relations:

$$z_\mathrm{c} = z + \varepsilon_z, \quad \varepsilon_z \sim N\left(0\,,\, \sigma_z^2\right) \tag{9}$$

$$Q_\mathrm{c} = Q + \varepsilon_Q, \quad \varepsilon_Q \sim N\left(0\,,\, (\sigma_Q Q)^2\right) \tag{10}$$

where z_c (m) and Q_c (m^3 s^{-1}) are the corrupted values of z(m) and Q (m^3 s^{-1}), ε_z (m) and ε_Q (m^3 s^{-1}) are the normally distributed errors with parameters σ_z (m) and σ_Q (%) of z and Q, respectively. The formulation of discharge errors allows representing larger uncertainties for high stage levels than for low flows due to uncertainties in discharge rating curves, as pointed out by Clark et al. (2008). Alternatively, simulated and observed discharges were also transformed into the log space before the assimilation, following Clark et al. (2008). In this case, observation errors were modeled by:

$$Q_\mathrm{c} = \varepsilon'_Q Q, \quad \varepsilon'_Q \sim \log N\left(1, {\sigma'_Q}^2\right) \tag{11}$$

where now ε'_Q is a log-normally distributed error with unit mean and standard deviation σ'_Q (%), similar to Eq. (10). At log space, standard deviation is given by $\sigma'_{\log Q} = \sqrt{\log\left({\sigma'_Q}^2 + 1\right)}$.

3 Experimental design

3.1 The Amazon River basin

The study area is the Amazon River basin, known as the largest hydrological system of the world (~ 6 million km^2 of surface area) and contributing with ~ 15 % to the total fresh water released into the oceans. The Amazon basin is characterized by extensive seasonally flooded areas (Hess et al., 2003; Papa et al., 2010b; Melack and Hess, 2010), which store and release large amounts of water from the rivers and consequently attenuate and delay flood waves in several days or months (Paiva et al., 2012a, 2013; Yamazaki et al., 2011). Also, complex river hydraulics are present, where the low river slopes cause backwater effects that control part of river dynamics (Meade, 1991; Trigg et al., 2009; Tomasella et al., 2010; Paiva et al., 2012a, 2013). Additionally, this region presents high precipitation rates (average ~ 2200 mm yr^{-1}) with high spatial variability and contrasting rainfall regimes in the northern (rainfall peak at JJA) and southern (rainfall peak at DJF) parts of the basin, with more defined wet and dry seasons occurring in southern and eastern regions (Espinoza et al., 2009).

3.2 Model implementation

We used a MGB-IPH implementation on the Amazon basin developed by Paiva et al. (2013), as briefly described below. The model was forced using meteorological data obtained from the CRU CL 2.0 dataset (New et al., 2002) and remotely sensed precipitation estimates from the TRMM 3B42 v6 product (Huffman et al., 2007), with spatial resolution of $0.25^{\circ} \times 0.25^{\circ}$ and daily time step for a period spanning 12 yr (1998–2009). The model parameters related to soil water budget were calibrated using daily discharge data from stream gauges (see next section for description of gauged data). Then, the model was validated against daily discharge and water level data from stream gauge stations, water levels derived from ENVISAT satellite altimetry data (Santos da Silva et al., 2010) (212 sites with 35-day repeat orbit), monthly Terrestrial Water Storage from GRACE mission (Frappart et al. 2010, 2011b) and monthly flood inundation extent from Papa et al. (2010b). Simulations agreed with observations, with relatively high Nash and Suttcliffe index (E_{NS}) values: $E_{NS} > 0.6$ in ~ 70 % of discharge gauges, $E_{NS} > 0.6$ in ~ 60 % of the water level stations derived from satellite altimetry, $E_{NS} = 0.71$ for total flood extent and $E_{NS} = 0.93$ for terrestrial water storage.

Since this study aimed at applications of data assimilation to hydrological forecasting, we also used a real time precipitation product to force the MGB-IPH model. We choose to use the TRMM Merge product (Rozante et al., 2010), which is a near to real time precipitation estimate based on TRMM 3B42RT (Huffman et al., 2007) merged with data from in situ gauges and provided by the Brazilian center for weather forecasts and climate studies CPTEC (*Centro de Previsão do Tempo e Estudos Climáticos*), a division of the Brazilian National Institute for Space Research INPE (*Instituto Nacional de Pesquisas Espaciais*).

3.3 Discharge and water level observations

We evaluated the assimilation of three types of data: (1) in situ discharge observations; (2) remotely sensed water levels derived from the ENVISAT radar altimeter; and (3) remotely sensed discharge estimates derived from radar altimetry water levels and rating curves.

In situ daily discharge from 109 stream gauges were provided by the Brazilian agency for water resources ANA (*Agência Nacional das Águas*), the Peruvian and Bolivian national meteorology and hydrology services SENAMHI (*Servicio Nacional de Meteorología e Hidrología*) and the French ORE-HYBAM program (*Hydrologie, Biogeochimie and Geodynamique du Bassin Amazonien*, http://www.ore-hybam.org). We also used stage data from 66 ANA gauge stations, but only for validation purposes.

Remotely sensed water levels were obtained from the ENVISAT satellite altimeter. The ENVISAT satellite has a 35-day repeat orbit and an 80 km inter-track distance at the Equator. The database used is an extension of the one presented in Santos da Silva et al. (2010), consisting in 212 altimetry stations (AS – deduced from the intersection of a satellite track with a water body) with water level time series for the 2002–2009 period. ENVISAT data selection techniques preconized by Santos da Silva et al. (2010) result in ~ 10 to 40 cm water level accuracy. Due to differences in water levels datum reference, the comparisons between simulated and observed water levels were performed in terms of anomalies, i.e. after removing the long-term average.

Discussion Paper | Discussion Paper | Discussion Paper | Discussion Paper |

Altimetry-based discharge data was developed by Getirana and Peters-Lidard (2013) for the Amazon basin, following the methodology first presented by Leon et al. (2006) in the Negro River sub-basin. This dataset was constructed using a rating-curve-based methodology deriving water discharge from ENVISAT altimetry data at 475 altimetric stations (AS). The stage-discharge relations at each AS were built based on satellite altimetry and outputs from a global flow routing (GFR) scheme (Getirana et al., 2012). A second experiment was performed in this study using observed discharges at gauge stations to force the GFR scheme at downstream reaches. Validation of the methodology against observed discharges at 90 sites showed a mean relative error of 27 % for the experiment using in situ discharge within the GFR scheme. We assimilated data only from the 287 ASs located downstream of a gauging station where results were improved in the second experiment.

3.4 Parameters of the DA scheme

The first sensitivity experiments used the following standard parameters of the DA scheme. Ensemble size of the EnKF was set as $N = 200$. Precipitation fields were corrupted considering the following error parameters: precipitation relative error $E = 25\,\%$, and precipitation relative bias $\beta = 1.0$ following Andreadis and Lettenmaier (2006); temporal decorrelation length of precipitation errors $\tau_t = 10$ days; and spatial decorrelation length of precipitation errors $\tau_x = 1.0^{\circ}$, similarly to Andreadis and Lettenmaier (2006) and Clark et al. (2008). The parameter of water level measurements error was set as $\sigma_z = 0.20$ m, based on the accuracy of ENVISAT estimates provided by Santos da Silva et al. (2010). We computed the mean relative error between in situ discharge measurements and values provided by rating curves at 87 gauging stations from the ANA database as a surrogate of the discharge error parameter σ_Q. The median value of all stations was 13 %, while Clark et al. (2008) used 10 % in its DA experiments. Therefore, we choose to also use $\sigma_Q = 10\,\%$ for simplicity. We used $\sigma_Q = 27\,\%$ for assimilation of satellite based discharge data, based on the error value found in Getirana and Peters-Lidard (2013).

3.5 Data assimilation experiments

We performed three data assimilation experiments, namely: (i) in situ discharge assimilation (Exp 1) (ii) radar altimetry assimilation (Exp 2) and (iii) assimilation of discharge series based on satellite altimetry (Exp 3).

In the first experiment, we tested: (Exp. 1a) the assimilation of discharge from almost all gauge stations (80 %) using a few of them for validation (20 %); (Exp. 1b) the assimilation of only 12 stations (~ 10 %) located at some of the major tributaries to emulate the situation of using only telemetric stream gauges for real time applications; (Exp. 1c) the assimilation of discharge from almost all gauge stations, similar to (Exp. 1a), but without transforming discharge into the log space (Sect. 2.4). Moreover, we explored the sensibility of the DA scheme to some of its parameters, namely the ensemble size N, precipitation relative error E and temporal and spatial decorrelation lengths of precipitation errors τ_t, and τ_x.

The second experiment (Exp. 2) evaluated the assimilation of ENVISAT radar altimetry water level anomalies. Stage data from in situ gauges were used for model verification. Simulations were also compared in terms of discharge using in situ data to evaluate the impact of water level assimilation in discharge estimates.

In the third experiment (Exp. 3), we assessed the assimilation of discharge derived from radar altimetry water level. Discharge data from stream gauges were used for verification.

In all cases, simulations started in 1998 and ran to 2002 for model spin-up. The year of 2003 was used for the spin-up of the DA scheme, where no update was performed in the first months allowing the system to develop a coherent correlation structure, following Andreadis and Lettenmaier (2006). Results were evaluated for the two year period 2004–2005 using the following performance statistics: (i) the Nash-Suttcliffe coefficient E_{NS} ranging from $-\infty$ to 1 (optimum) and (ii) changes in root mean square error Δrms ranging from $-100\,\%$ (optimum) to ∞.

3.6 Prospects of streamflow forecasting

Hindcast streamflow forecasts were generated using an ensemble streamflow prediction (ESP) approach (Day, 1985), as described below. The model uses an estimate of initial conditions derived from the DA scheme and runs forced by an ensemble of observed meteorological data from past years. An estimate of initial conditions is computed during the spin-up period using a hydrological model driven by observed meteorological forcings, updated using data assimilation of observations up to the time of forecast (e.g. forecast starts with model states from 1 June 2010). Then, an ensemble forecast is obtained using observed meteorological data resampled from past years (e.g. meteorological data from 1 June to 1 September of years 1998, 1999, ..., 2009).

Precipitation from TRMM Merge was used during spin-up period, while during forecast the model was forced with TRMM 3B42 data for the period spanning 12 yr (1998–2009) and, consequently, the forecast ensemble had 12 members. The DA scheme used the configuration from Exp. 1b where in situ discharge data were assimilated to update model states before starting a forecast. ESP runs generated decadal forecasts up to 90 days lead time and starting at every 1st, 10th and 20th day of the month for the two year period of 2004–2005.

For simplicity reasons, forecasts were evaluated only by deterministic means by averaging ensemble values into a single forecast. We used the skill score SS_{cli} which compares the performance of the model forecasts with a control forecast based on climatology (Wilks, 2006):

$$SS_{cli} = 1 - \frac{\sum_t (Q_{obs}^t - Q_{for}^t)^2}{\sum_t (Q_{obs}^t - Q_{cli}^t)^2} \tag{12}$$

where t is the time interval, Q_{obs} is daily discharge observed at stream gauge stations, Q_{for} is forecasted discharge, Q_{cli} is the climatological value of discharge on day t

computed from observations. SS_{cli} ranges from $-\infty$ to 1 (optimum) and positive values show an improvement over a forecast based on climatology.

4 Results and discussion

4.1 In situ discharge assimilation

We start our analysis evaluating the sensibility of the DA scheme performance in terms of Δrms to some of its parameters, as presented in Fig. 1. The objective of such examination is to verify which parameters are the most important ones and if the DA performance is improved by using values of these parameters that are different from the first guess ones based on previous studies (see Sect. 3.4). The configuration of Exp. 1a was used, where in situ discharge data were assimilated. Results were evaluated in terms of mean changes in root mean squared error (Δrms) between observed and simulated discharges, computed for two samples, the first including stream gauges used for data assimilation and the latter only the validation ones. Larger decreases in the rms error indicate better performance of the DA scheme.

According to the analysis, the DA scheme strongly depends on the ensemble size N. Small N values produce small improvements in discharge results and larger values enhance the DA performance (smaller Δrms values), although the improvement rate is small for N values larger than 150 members. Such behaviour is possibly due to numerical reasons, since a larger N enable a better sampling of model covariance errors from the ensemble, as discussed by Evensen (2009). The DA scheme is also very sensitive to precipitation relative error E and increasing E values improves DA performance. However, if E is larger than 50 %, Δrms increases in validation sites causing worse results (see Fig. 1). Possibly, larger precipitation errors cause larger model uncertainty and consequently the DA scheme gives more weight to observations, but it starts to degrade model results at different locations after some point. A moderate dependence to the τ_x parameter was found and spatial correlation of precipitation errors showed to be of importance, since the performance degrades for smaller decorrelation lengths. The best results were obtained for 1.5° for both the assimilation and validation samples. Finally, a weak sensibility to the τ_t parameter was found, which indicates that considering temporal correlation in precipitation errors is not as important as spatial correlation.

Based on the sensitivity tests, we used the following new parameter values for the further experiments: $N = 200$ (unchanged), $E = 50\,\%$, $\tau_x = 1.5°$ and $\tau_t = 10$ days (unchanged). However, it is noteworthy that these parameter values related to precipitation errors, although providing better results for data assimilation, may not realistically represent errors in the TRMM Merge dataset or the spatially variable satellite precipitation errors presented in Tian and Peters-Lidard (2010). That is possibly because we considered that model uncertainty comes from precipitation errors and neglected other sources such as parameter and model structural errors (Liu and Gupta, 2007). Therefore, and since the first guess values were not fully justified in the previous studies (Andreadis and Lettenmaier, 2006; Clark et al., 2008), we preferred to use the parameter values where the DA scheme performs better.

We first evaluate results from the Exp. 1a. The DA scheme improves results by decreasing model errors in almost all stream gauges (blue sites in Fig. 2a), including both assimilation and validation sites. On average, E_{NS} values increase from 0.71 to 0.94 and the rms error decreases by 49 % (Table 1). For example, at an assimilation site located on the Negro River (Fig. 3a), when the EnKF is used, the discharge estimates are much closer to observations if compared with the open-loop simulation. The E_{NS} index increases from 0.62 to 0.91 and the rms error decreases by 51 %. Similarly, results also improve at validation sites, although with a smaller degree, and the E_{NS} index increases from 0.60 to 0.73, with a reduction in rms error of −16 % (Table 1), as illustrated at a validation site located at upper Juruá River basin (Fig. 3b). Such results demonstrate that the DA scheme improves model discharge estimates, not only at sites where data were assimilated but possibly at ungauged rivers reaches as well.

In Exp. 1b, results improve at assimilation sites $-E_{NS}$ increases from 0.89 to 0.98 and the rms error decreases by 50 % (Table 1). However, since data from only a few

gauges were assimilated, there is no important improvement (Δrms = −3 %) if all validation sites are examined together. As expected, according to Fig. 2b the DA scheme improves discharge estimates mostly at large rivers (e.g. Fig. 3c), where E_{NS} increases from 0.79 to 0.87 while Δrms equals −23%. But at smaller rivers, in most cases the DA scheme has minor effect on simulated discharges (green squares at Fig. 2b) or in some cases it degrades results.

In previous studies conducted over smaller basins (e.g. in Clark et al., 2008; and in others summarised by Lee et al., 2012), the attempt to transfer information to neighbour or upstream ungauged river reaches was unsuccessful and corrupted model results, while in our case (Exp. 1b) the DA scheme degraded model outputs mostly at smaller basins and improved results at larger rivers. Such behaviour possibly happens because the state estimation in distributed hydrological models is subject to overfitting due to the large dimensionality of the model state space, and consequently, when limited data is available, the data assimilation may update state variables at some lumped fashion such as the sub-basin scale, as explained by Lee et al. (2012).

Finally, we compare the use (Exp. 1a) or not (Exp. 1c) of the transformation of discharge values into the log space before data assimilation. The performance of the DA scheme degrades if the log transformation is not used, and in this case Δrms increases to −29 % and −10 % for the assimilation and validation samples, respectively, instead of the −49 % and −16 % values obtained in the Exp. 1a. Clark et al. (2008) argue that the EnKF with log transformation performs better because relationships between streamflow and model states are non-linear and state updates are exceptionally large when differences between model and observed values are high. However, the worst performance was observed mostly at smaller river reaches (see Fig. 2c) as illustrated in Fig. 3c. Also, DA performs better at gauging stations in large rivers and Δrms increases from −34 % (Exp. 1a) to −40 % (Exp. 1c). Apparently, when the log transformation is not used, the DA scheme gives more weight to large discharge values ($\sim 10^3$ to $\sim 10^5\,m^3\,s^{-1}$) at large rivers while observations at the smaller ones ($<\sim 10^3\,m^3\,s^{-1}$) are not fully taken into account. These results indicate the importance of using the log

Discussion Paper | Discussion Paper | Discussion Paper | Discussion Paper |

space transformation also to deal with very different discharge magnitudes, including the ones arising from different spatial scales but also concerning to flood and drought flows.

4.2 Radar altimetry data assimilation

In this section, the assimilation of water levels derived from ENVISAT altimetry is evaluated (Exp. 2). Stage and discharge data observed at in situ gauging stations were used for validation purposes.

The DA scheme improves water level simulations at altimetry stations used for assimilation (Fig. 4a), as illustrated in Fig. 5a. On average, rms decreases by 56 % and E_{NS} values increase from 0.66 to 0.96 (Table 2). Simulated water level accuracy also increases when compared to in situ stage data (Δrms = −13 %). However, the improvement is more evident if only gauging stations located at rivers where altimetry data were assimilated (Figs. 4b and 5b). In this case, mean Δrms equals −43 % and E_{NS} changes from 0.75 to 0.94 (Table 2), similar to what was obtained at altimetry stations. At other sites, the DA scheme has a minor effect on simulated water levels or even degrades results in some cases. Similar results were found for the in situ discharge validation sample (Fig. 4c). Assimilating water level data improves discharge estimates (Δrms = −15 %) mostly at the same rivers in which altimetry data is available (e.g. Fig. 5c). But it also degrades results at some of the other river reaches.

Furthermore, the DA scheme can degrade results in some reaches where no data were assimilated. Such a problem is possibly caused by spurious correlations in the model covariance matrix from the EnKF due to a poor sampling from the ensemble. Aiming to avoid spurious correlations, methods such as covariance localization or local analysis (Sakov and Bertino, 2010) could be used to constrain the influence of observations based on distance criteria as already used in atmospheric or ocean applications. However, in our view, a particular localization criteria should be developed for hydrological applications, since the correlation between the model states can be a function

of an Euclidean distance in some cases (e.g. soil moisture) or in others, of a distance measured following the rivers' path (e.g. river discharge and water levels).

Results from this experiment demonstrate that the assimilation of radar altimetry data into large scale hydrologic models can improve simulations, mainly in terms of water levels but also in discharge. Even though ENVISAT data is provided at a 35-day temporal resolution, its assimilation can improve model results at a daily basis as illustrated in Fig. 5b, c possibly due to the low temporal variability of Amazonian hydrographs and the fact that ENVISAT measurements are non-simultaneous.

4.3 Assimilation of discharge series based on satellite altimetry

In the last DA experiment (Exp. 3), we evaluate the assimilation of discharge data derived from ENVISAT water level. Therefore, the data assimilated into the model has the same high spatial coverage and low temporal sampling as altimetry water levels have, but it also contains discharge information which is the most important hydrological variable of the model. In situ discharge data were also used for validation.

The DA scheme was able to assimilate altimetry-based discharges increasing the agreement between these observations and model results in most of the altimetry stations (Fig. 6a), as exemplified in Fig. 7a. In average, the rms error between altimetry-based discharges and model results decreased 23 % (Table 3), which represents a smaller improvement if compared to the assimilation of in situ discharge (Δrms = −49 % in Exp. 1a). Since observation errors are larger in the altimetry-based discharges, the DA scheme gives more weight to background model results and updated discharge values are not so close to measurements. The comparison of model results with in situ discharge data (Fig. 6b) shows that errors decrease mostly at gauging stations located at rivers where altimetry data were assimilated (e.g. Fig. 7b). At these sites, E_{NS} changes from 0.76 to 0.80 and the mean Δrms is −14 % (Table 3), which is comparable to the improvement obtained in the altimetry data assimilation (Exp. 2, Table 2) over discharge results (Δrms = −15 %), but smaller than the enhancement of water level results (Δrms = −43 %). Moreover, similarly to Exp. 2, at gauging stations located outside the assimilation domain, the DA scheme has a minor effect on simulated discharge or degrades results in some cases.

Results from this section show the potential of assimilating discharge data derived from satellite altimetry into large scale hydrological models instead of in situ discharge or satellite water levels, even though such data has lower temporal resolution and accuracy if compared to data gathered at in situ gauging stations.

4.4 Prospects of streamflow forecasting

We now assess the potential of a large scale hydrologic-hydrodynamic model coupled with a DA scheme to provide streamflow forecasts in the Amazon basin. Since hydrological initial states governs discharge predictability at the large Amazonian rivers (discussed by Paiva et al., 2012b), we have chosen to generate forecasts starting with initial states gathered by the DA scheme and then using the ensemble streamflow prediction approach – ESP (Day, 1985), where the model is run forced by an ensemble of observed meteorological data from past years. Since this is a first attempt, we have chosen to evaluate forecasts using only the DA scheme configuration from Exp. 1b, where the model is updated using discharge data from 12 gauging stations located on the Amazon and its main tributaries.

We first evaluate hindcast forecasts at the Solimões/Amazon mainstem, including upper Solimões River at Tamishiyacu, Solimões River at Manacapuru and Amazon River at Óbidos (Fig. 8). The model was able to forecast discharges with relatively high accuracy even for very large lead times (90 days). In all cases, forecasts are markedly better than simply using discharge climatology, as shown by positive values of SS_{cli} skill score (Fig. 8). As expected, the agreement between model values and observations decreases as function of lead time, and, for example, SS_{cli} decreases from 0.90 to 0.49 for forecasts 10 and 90 days ahead at Óbidos station. But it remains very high, showing that it would be possible to produce accurate forecasts at the Amazon main river for even larger lead times. Model performance also increases from the upper to the lower part of the Solimões/Amazon River, and at the same time, the spread of the ESP

ensemble at large lead times increases upstream and decreases downstream. Such behaviour is explained by the fact that in larger rivers, the hydrological predictability is much more influenced by the current volumes of water stored upstream than by future precipitation forcing, as discussed by Paiva et al. (2012b).

Analysis from Fig. 8 also demonstrates that the model successfully predicted the severe 2005 drought at the Solimões/Amazon main stem. At this year, discharges dropped ~ 1 month earlier than normal (Fig. 8) and river levels fell to historically low levels causing navigation to be suspended (Marengo et al., 2008). Even so, the model was able to predict this low flows ~ 90 days ahead.

We now evaluate forecasts at gauging stations located all over the Amazon basin. Forecasts for a smaller lead time of 5 days or even 15 days (Fig. 9a, b) were relatively accurate with positive SS_{cli} values at several gauging stations located at both upstream and downstream rivers. However, the quality of the forecasts decreased as a function of lead time (30 and 90 days, Fig. 9c, d). It becomes very poor at smaller rivers and remains meaningful with positive SS_{cli} values mainly at gauging stations with large draining areas. For 90 days lead time, SS_{cli} index remains positive at almost all stations along the Solimões/Amazon main stem and in some of the main tributaries. This behavior is also illustrated at Fig. 10. SS_{cli} values are usually higher at gauging stations located in rivers draining large areas and decrease with lead time. For instance, if only stations gauging rivers with drainage area larger than $10^5\,km^2$ or $4 \times 10^5\,km^2$ are considered, on average, forecasts remain better than climatology ($SS_{cli} > 0$) up to ~ 15 and ~ 25 days lead time, respectively. On the other hand, if only the largest rivers are taken into account ($> 10^6\,km^2$), SS_{cli} values are high and always positive, which demonstrates the good performance of the model forecasts. SS_{cli} is also high at stream gauges used for data assimilation where forecasts are usually better, SS_{cli} is close to one for small lead times, as expected, and becomes negative after ~ 55 days.

Discussion Paper | Discussion Paper | Discussion Paper | Discussion Paper |

5 Summary and conclusions

We presented the development and evaluation of a data assimilation scheme for both gauged and satellite altimetry-based discharge and water levels into a large scale hydrologic-hydrodynamic model of the Amazon River basin using the Ensemble Kalman Filter – EnKF. We also evaluated hindcast forecasts based on this system using the ensemble streamflow prediction approach, where the model was forced by an ensemble of past precipitation forcing from TRMM mission.

According to our results, the data assimilation scheme performed well in assimilating in situ and remotely sensed discharge and water levels into the large scale hydrologic-hydrodynamic model. The assimilation of in situ discharge showed that EnKF can improve discharge estimates at assimilation gauges but, differently from previous studies at smaller basins (e.g. Clark et al., 2008; and others summarised by Lee et al., 2012), also transfer information to ungauged rivers by improving results at validation sites, although with a smaller degree. The assimilation of discharge data at a reduced number of gauging stations located at larger rivers improves results mostly at the large reaches but it degrades results at some smaller basins. Also, the transformation of discharge measurements into the log space proved to be important to deal with very different discharge magnitudes arising from different spatial scales or from contrasting flood and recession flows.

The assimilation of satellite altimetry data improved model water levels, and also discharges, mostly at the same river reaches where altimetry stations are located. Assimilating altimetry-based discharge also improved model estimates, although with minor degree if compared to the in situ discharge assimilation, probably due to the larger errors in remotely sensed observations. However, in both cases, even though radar altimetry data has low temporal resolution (35 days), its assimilation can improve model results at a daily basis, possibly due to its higher spatial resolution and the low temporal variability of Amazonian hydrographs.

The sensitivity analysis of the parameter from the DA scheme highlighted the importance of the magnitude of precipitation errors and that of their spatial correlation, while temporal correlation showed to be dispensable.

The deterioration of model performance at some unmonitored reaches may be due to the large dimensionality of state space in distributed hydrological models compared to the available information. Consequently, data assimilation may update state variables at some lumped fashion such as the sub-basin scale, as explained by Lee et al. (2012). This problem can be also due to spurious correlations that can arise by numerical reasons and could be avoided by using proper spatial localization methods (e.g. Sakov and Bertino, 2010) developed for hydrological applications to constrain the influence of measurements. Additionally, the DA scheme could benefit from a better characterization of model errors, where not only precipitation but other sources of uncertainty, such as in model parameters and structure could be included, as suggested by Liu et al. (2012).

Although limitations still exist, results are encouraging. This kind of DA scheme could also be easily employed to other similar regional/global scale hydrological models (e.g. Yamazaki et al., 2011; Decharme et al., 2012; Alfieri et al., 2012). It has also the potential to improve by assimilating remotely sensed water levels gathered by other satellite missions as the existing ones, or the altimetry missions to be launched in the coming years by the European Spatial Agency ESA, namely the Sentinel-3 constellation and the forthcoming SWOT mission (Durand et al., 2010a). Moreover, the altimetry-based discharge assimilation can improve when better discharge estimates become available, such as the ones under development for the future SWOT mission (Durand et al., 2010b).

Finally, the model was able to provide relatively accurate streamflow forecasts in the Amazon basin. For smaller lead times (~ 5 to 15 days), forecasts agreed with observations in lots of gauging stations and for larger lead times (> 30 days) they remained meaningful mostly at larger rivers. Forecasts were usually better at stream gauges used for data assimilation, especially for smaller lead times. Along the Solimões/Amazon main stem, forecast were highly accurate even for very large lead times (90 days) and the model was capable to successfully predict the record 2005 drought at the Solimões/Amazon River well in advance. These results demonstrate the potential for developing stream flow forecasts with large lead times at the world's large river basins, such as the Amazon, founded on large scale hydrological models based mostly on initial states gathered with proper DA schemes, and using past climate with the ESP approach. Also, results point to the potentiality of providing hydrological forecasts at poorly monitored regions by using mostly remotely sensed information.

Acknowledgements. The authors are grateful for: the financial and operational support from the Brazilian agencies FINEP and ANA ("*Projeto de Integração e Cooperação Amazônica para a Modernização do Monitoramento Hidrológico*" ICA-MMH) and CNPq-IRD ("*Assimilação de Dados de monitoramento Espacial para a análise do regime hidrológico da Bacia Amazônica e a previsão de curto e médio prazos*"); the ENVISAT satellite altimetry data supplied by ESA; the TRMM data supplied by NASA and associated agencies; the TRMM Merge data provided by CPTEC/INPE; the discharge and stage data provided by ANA, Hybam, SENHAMI-Peru and SENHAMI-Bolivia; the EnKF Fortran codes provided by Geir Evensen; the support from Fernando Fan in processing precipitation data; as well as for the constructive comments from Adalberto Meller and Jeffrey Neal.

INSU
Institut national des sciences de l'Univers

The publication of this article is financed by CNRS-INSU.

References

Alfieri, L., Burek, P., Dutra, E., Krzeminski, B., Muraro, D., Thielen, J., and Pappenberger, F.: GloFAS – global ensemble streamflow forecasting and flood early warning, Hydrol. Earth Syst. Sci. Discuss., 9, 12293–12332, doi:10.5194/hessd-9-12293-2012, 2012.

Alsdorf, D. E., Rodríguez, E., and Lettenmaier, D. P.: Measuring surface water from space, Rev. Geophys., 45, RG2002, doi:10.1029/2006RG000197, 2007.

Andreadis, K. M. and Lettenmaier, D. P.: Assimilating remotely sensed snow observations into a macroscale hydrology model, Adv. Water Resour., 29, 6, 872–886, 2006.

Andreadis, K. M., Clark, E. A., Lettenmaier, D. P., and Alsdorf, D. E.: Prospects for river discharge and depth estimation through assimilation of swath-altimetry into a raster-based hydrodynamics model, Geophys. Res. Lett., 34, L10403, doi:10.1029/2007GL029721, 2007.

Biancamaria, S., Durand, M., Andreadis, K. M., Bates, P. D., Boone, A., Mognard, N. M., Rodriguez, E., Alsdorf, D. E., Lettenmaier, D. P., and Clark, E. A.: Assimilation of virtual wide swath altimetry to improve Arctic river modeling, Remote Sens. Environ., 115, 373–381, 2011.

Chen, J. L., Wilson, C. R., and Tapley, B. D.: The 2009 exceptional Amazon flood and interannual terrestrial water storage change observed by GRACE, Water Resour. Res., 46, W12526, doi:10.1029/2010WR009383, 2010.

Clark, M. P., Rupp, D. E., Woods, R. A., Zheng, X., Ibbitt, R. P., Slater, A. G., Schmidt, J., and Uddstrom, M. J.: Hydrological data assimilation with the ensemble Kalman filter: use of streamflow observations to update states in a distributed hydrological model, Adv. Water Res., 31, 1309–1324, doi:10.1016/j.advwatres.2008.06.005, 2008.

Coe, M. T., Costa, M. H., and Howard, E. A.: Simulating the surface waters of the Amazon River basin: impacts of new river geomorphic and flow parameterizations, Hydrol. Process., 22, 2542–2553, 2008.

Collischonn, W., Allasia, D. G., Silva, B. C., and Tucci, C. E. M.: The MGB-IPH model for large-scale rainfall-runoff modeling, Hydrolog. Sci. J., 52, 878–895, 2007.

Day, G. N.: Extended streamflow forecasting using NWSRFS, J. Water Resour. Pl.-ASCE, 111, 157–170, 1985.

Decharme, B., Alkama, R., Papa, F., Faroux, S., Douville, H., and Prigent, C.: Global off-line evaluation of the ISBA-TRIP flood model, Clim. Dynam., 38, 1389–1412, doi:10.1007/s00382-011-1054-9, 2012.

Durand, M., Andreadis, K. M., Alsdorf, D. E., Lettenmaier, D. P., Moller, D., and Wilson, M.: Estimation of bathymetric depth and slope from data assimilation of swath altimetry into a hydrodynamic model, Geophys. Res. Lett., 35, L20401, doi:10.1029/2008GL034150, 2008.
Durand, M., Fu, L. L., Lettenmaier, D. P., Alsdorf, D. E., Rodríguez, E., and Fernandez, D. E.: The surface water and ocean topography mission: observing terrestrial surface water and oceanic submesoscale eddies, Proc. IEEE, 98, 766–779, 2010a.
Durand, M., Rodríguez, E., Alsdorf, D., and Trigg, M.: Estimating river depth from remote sensing swath interferometry measurements of river, IEEE J. Sel. Top. Appl., 3, 20–31, 2010b.
Espinoza, J. C., Ronchail, J., Guyot, J. L., Cocheneau, G., Filizola, N., Lavado, W., de Oliveira, E., Pombosa, R., and Vauchel, P.: Spatio-Temporal rainfall variability in the Amazon Basin Countries (Brazil, Peru, Bolivia, Colombia and Ecuador), Int. J. Climatol., 29, 1574–1594, 2009.
Espinoza, J. C., Ronchail, J., Guyot, J. L., Junquas, C., Vauchel, P., Lavado, W., Drapeau, G., and Pombosa, R.: Climate variability and extreme drought in the upper Solimões River (western Amazon Basin): understanding the exceptional 2010 drought, Geophys. Res. Lett., 38, L13406, doi:10.1029/2011GL047862, 2011.
Evensen, G.: The ensemble Kalman filter: theoretical formulation and practical implementation, Ocean Dynam., 53, 343–367, 2003.
Evensen, G.: Sampling strategies and square root analysis schemes for the EnKF, Ocean Dyn., 54, 539–560, 2004.
Evensen, G.: Data assimilation, The Ensemble Kalman Filter, 2nd Edn., Springer, 2009.
Farr, T. G., Caro, E., Crippen, R., Duren, R., Hensley, S., Kobrick, M., Paller, M., Rodriguez, E., Rosen, P., Roth, L., Seal, D., Shaffer, S., Shimada, J., Umland, J., Werner, M., Burbank, D., Oskin, M., and Alsdorf, D.: The shuttle radartopography mission, Rev. Geophys., 45, RG2004, doi:10.1029/2005RG000183, 2007.
Frappart, F., Ramillien, G., Maisongrande, P., and Bonnet, M.-P.: Denoising satellite gravity signals by Independent Component Analysis, IEEE Geosci. Remote S., 7, 421–425, doi:10.1109/LGRS.2009.2037837, 2010.
Frappart, F., Ramillien, G., Leblanc, M., Tweed, S. O., Bonnet, M.-P., and Maisongrande, P.: An independent component analysis approach for filtering continental hydrology in the GRACE gravity data, Remote Sens. Environ., 115, 187–204, doi:10.1016/j.rse.2010.08.017, 2011.
Gedney, N., Cox, P. M., and Huntingford, C.: Climate feedback from wetland methane emission, Geophys. Res. Lett., 31, L20503, doi:10.1029/2004GL020919, 2004.

Getirana, A. C. V. and Peters-Lidard, C.: Estimating water discharge from large radar altimetry datasets, Hydrol. Earth Syst. Sci., 17, 923–933, doi:10.5194/hess-17-923-2013, 2013.
Getirana, A. C. V., Boone, A., Yamazaki, D., Decharme, B., Papa, F., and Mognard, N.: The hydrological modeling and analysis platform (HyMAP): evaluation in the Amazon basin, J. Hydrometeorol., 13, 1641–1665, doi:10.1175/JHM-D-12-021.1, 2012.
Hess, L. L., Melack, J. M., Novo, E. M. L. M., Barbosa, C. C. F., and Gastil, M.: Dual-season mapping of wetland inundation and vegetation for the central Amazon basin, Remote Sens. Environ., 87, 404–428, 2003.
Huffman, G., Adler, R., Bolvin, D., Gu, G., Nelkin, E., Bowman, K., Hong, Y., Stocker, E., and Wolff, D.: The TRMM multisatellite precipitation analysis (TCMA): quasi-global, multiyear, combined-sensor precipitation estimates at fine scales, J. Hydrometeorol., 8, 38–55, 2007.
Kalman, R. E.: A new approach to linear filtering and prediction problems, T. AMSE J. Basic Engin., 82, 35–45, 1960.
Krinner, G.: Impact of lakes and wetlands on boreal climate, J. Geophys. Res., 108, 4520, doi:10.1029/2002JD002597, 2003.
Kumar, S. V., Reichle, R. H., Peters-Lidard, C. D., Koster, R. D., Zhan, X., Crow, W. T., Eylander, J. B., and Houser, P. R.: A land surface data assimilation framework using the land information system: description and applications, Adv. Water Resour., 31, 1419–1432, doi:10.1016/j.advwatres.2008.01.013, 2008.
Lee, H., Seo, D.-J., and Koren, V.: Assimilation of streamflow and in situ soil moisture data into operational distributed hydrologic models: effects of uncertainties in the data and initial model soil moisture states, Adv. Water Resour., 34, 1597–1615, doi:10.1016/j.advwatres.2011.08.012, 2011.
Lee, H., Seo, D.-J., Liu, Y., Koren, V., McKee, P., and Corby, R.: Variational assimilation of streamflow into operational distributed hydrologic models: effect of spatiotemporal scale of adjustment, Hydrol. Earth Syst. Sci., 16, 2233–2251, doi:10.5194/hess-16-2233-2012, 2012.
Leon, J. G., Calmant, S., Seyler, F., Bonnet, M.-P., Cauhopé, M., and Frappart, F.: Rating curves and average water depth at the Upper Negro river from satellite altimetry and modeled discharges, J. Hydrol., 328, 481–496, 2006.
Liu, Y. and Gupta, H. V.: Uncertainty in hydrologic modeling: toward an integrated data assimilation framework, Water Resour. Res., 43, W07401, doi:10.1029/2006WR005756, 2007.

Liu, Y., Weerts, A. H., Clark, M., Hendricks Franssen, H.-J., Kumar, S., Moradkhani, H., Seo, D.-J., Schwanenberg, D., Smith, P., van Dijk, A. I. J. M., van Velzen, N., He, M., Lee, H., Noh, S. J., Rakovec, O., and Restrepo, P.: Advancing data assimilation in operational hydrologic forecasting: progresses, challenges, and emerging opportunities, Hydrol. Earth Syst. Sci., 16, 3863–3887, doi:10.5194/hess-16-3863-2012, 2012.

Marengo, J., Nobre, C., Tomasella, J., Oyama, M., de Oliveira, G., de Oliveira, R., Camargo, H., and Alves, L.: The drought in Amazonia in 2005, J. Climate, 21, 495–516, 2008.

Marengo, J. A., Tomasella, J., Alves, L. M., Soares, W. R., and Rodriguez, D. A.: The drought of 2010 in the context of historical droughts in the Amazon region, Geophys. Res. Lett., 38, L12703, doi:10.1029/2011GL047436, 2011.

McMillan, H. K., Hreinsson, E. Ö., Clark, M. P., Singh, S. K., Zammit, C., and Uddstrom, M. J.: Operational hydrological data assimilation with the recursive ensemble Kalman filter, Hydrol. Earth Syst. Sci., 17, 21–38, doi:10.5194/hess-17-21-2013, 2013.

Meade, R. H., Rayol, J. M., Da Conceição, S. C., and Natividade, J. R. G.: Backwater effects in the Amazon River basin of Brazil, Environ. Geol. Water Sci., 18, 105–114, 1991.

Melack, J. M. and Hess, L. L.: Remote sensing of the distribution and extent of wetlands in the Amazon basin, in: Amazonian Floodplain Forests: Ecophysiology, Ecology, Biodiversity and Sustainable Management, edited by: Junk, W. J. and Piedade, M., Ecological Studies, Vol. 210, Part 1, Springer, 43–59, 2010.

Neal, J. C., Atkinson, P. M., and Hutton, C. W.: Flood inundation model updating using ensemble Kalman filter and spatially distributed measurements, J. Hydrol., 336, 401–415, 2007.

Neal, J. C., Schumann, G. J.-P., Bates, P. D., Buytaert, W., Matgen, P., and Pappenberger, F.: A data assimilation approach to discharge estimation from space, Hydrol. Process., 23, 3641–3649, doi:10.1002/hyp.7518, 2009.

New, M., Lister, D., Hulme, M., and Makin, I.: A high-resolution data set of surface climate over global land areas, Clim. Res., 21, 1–25, 2002.

Nijssen, B. and Lettenmaier, D.: Effect of precipitation sampling error on simulated hydrological fluxes and states: anticipating the Global Precipitation Measurement satellites, J. Geophys. Res., 109, D02103, doi:10.1029/2003JD003497, 2004.

Oki, T. and Kanae, S.: Global hydrological cycles and world water resources, Science, 313, 1068–1072, doi:10.1126/science.1128845, 2006.

Paiva, R. C. D., Collischonn, W., and Tucci, C. E. M.: Large scale hydrologic and hydrodynamic modeling using limited data and a GIS based approach, J. Hydrol., 406, 170–181, 2011.

Paiva, R. C. D., Collischonn, W., and Buarque, D. C.: Validation of a full hydrodynamic model for large scale hydrologic modelling in the Amazon, Hydrol. Process., 27, 333–346, doi:10.1002/hyp.8425, 2012a.

Paiva, R. C. D., Collischonn, W., Bonnet, M. P., and de Gonçalves, L. G. G.: On the sources of hydrological prediction uncertainty in the Amazon, Hydrol. Earth Syst. Sci., 16, 3127–3137, doi:10.5194/hess-16-3127-2012, 2012b.

Paiva, R. C. D., Collischonn, W., Bonnet, M.-P., Buarque, D. C., Frappart, F., Calmant, S., and Mendes, C. B.: Large scale hydrologic and hydrodynamic modelling of the Amazon River basin, Water Resour. Res., online first, doi:10.1002/wrcr.20067, 2013.

Papa, F., Durand, F., Rossow, W. B., Rahman, A., and Bala, S. K.: Satellite altimeter-derived monthly discharge of the Ganga-Brahmapoutra River and its seasonal to interannual variations from 1993 to 2008, J. Geophys. Res., 115, C12013, doi:10.1029/2009JC006075, 2010a.

Papa, F., Prigent, C., Aires, F., Jimenez, C., Rossow, W. B., and Matthews, E.: Interannual variability of surface water extent at the global scale, 1993–2004, J. Geophys. Res., 115, D12111, doi:10.1029/2009JD012674, 2010b.

Pereira-Cardenal, S. J., Riegels, N. D., Berry, P. A. M., Smith, R. G., Yakovlev, A., Siegfried, T. U., and Bauer-Gottwein, P.: Real-time remote sensing driven river basin modeling using radar altimetry, Hydrol. Earth Syst. Sci., 15, 241–254, doi:10.5194/hess-15-241-2011, 2011, 2011.

Rakovec, O., Weerts, A. H., Hazenberg, P., Torfs, P. J. J. F., and Uijlenhoet, R.: State updating of a distributed hydrological model with Ensemble Kalman Filtering: effects of updating frequency and observation network density on forecast accuracy, Hydrol. Earth Syst. Sci., 16, 3435–3449, doi:10.5194/hess-16-3435-2012, 2012.

Reichle, R. H.: Data assimilation methods in the Earth sciences, Adv. Water Resour., 31, 1411–1418, doi:10.1016/j.advwatres.2008.01.001, 2008.

Reichle, R. H., Mclaughlin, D. B., and Entekhabi, D.: Hydrologic data assimilation with ensemble Kalman filter, Mon. Weather Rev., 130, 103–114, 2002.

Ricci, S., Piacentini, A., Thual, O., Le Pape, E., and Jonville, G.: Correction of upstream flow and hydraulic state with data assimilation in the context of flood forecasting, Hydrol. Earth Syst. Sci., 15, 3555–3575, doi:10.5194/hess-15-3555-2011, 2011.

Rozante, J. R., Moreira, D. S., de Goncalves, L. G. G., and Vila, D. A.: Combining TRMM and surface observations of precipitation: technique and validation over South America, Weather Forecast., 25, 885–894, doi:10.1175/2010WAF2222325.1, 2010.

Santos da Silva, J., Calmant, S., Seyler, F., Rotunno Filho, O. C., Cochonneau, G., and Mansur, W. J.: Water levels in the Amazon basin derived from the ERS 2 and ENVISAT radar altimetry missions, Remote Sens. Environ., 114, 2160–2181, 2010.

Thielen, J., Bartholmes, J., Ramos, M.-H., and de Roo, A.: The European Flood Alert System – Part 1: Concept and development, Hydrol. Earth Syst. Sci., 13, 125–140, doi:10.5194/hess-13-125-2009, 2009.

Thirel, G., Martin, E., Mahfouf, J.-F., Massart, S., Ricci, S., and Habets, F.: A past discharges assimilation system for ensemble streamflow forecasts over France – Part 1: Description and validation of the assimilation system, Hydrol. Earth Syst. Sci., 14, 1623–1637, doi:10.5194/hess-14-1623-2010, 2010.

Tian, Y. and Peters-Lidard, C. D.: A global map of uncertainties in satellite-based precipitation measurements, Geophys. Res. Lett., 37, L24407, doi:10.1029/2010GL046008, 2010.

Tomasella, J., Borma, L. S., Marengo, J. A., Rodriguez, D. A., Cuartas, L. A., Nobre, C. A., and Prado, M. C. R.: The droughts of 1996–1997 and 2004–2005 in Amazonia: hydrological response in the river main-stem, Hydrol. Process., 25, 1228–1242, doi:10.1002/hyp.7889, 2010.

Trigg, M. A., Wilson, M. D., Bates, P. D., Horritt, M. S., Alsdorf, D. E., Forsberg, B. R., and Vega, M. C.: Amazon flood wave hydraulics, J. Hydrol., 374, 92–105, 2009.

Uvo, C. B. and Graham, N. E.: Seasonal runoff forecast for northern South America: a statistical model, Water Resour. Res., 34, 3515–3524, doi:10.1029/98WR02854, 1998, 1998.

Uvo, C. B., Tölle, U., and Berndtsson, R.: Forecasting discharge in Amazonia using artificial neural networks, Int. J. Climatol., 20, 1495–1507, doi:10.1002/1097-0088(200010)20:12<1495::AID-JOC549>3.0.CO;2-F, 2000.

Vrugt, J. A., Diks, C. G. H., Gupta, H. V., Bouten, W., and Verstraten, J. M.: Improved treatment of uncertainty in hydrologic modeling: combining the strengths of global optimization and data assimilation, Water Resour. Res., 41, W01017, doi:10.1029/2004WR003059, 2005.

Wilks, D. S.: Statistical Methods in the Atmospheric Sciences, 2st ed., Academic Press, 467 pp., 2006.

Wilson, W., Bates, P., Alsdorf, D., Forsberg, B., Horritt, M., Melack, J., Frappart, F., and Famiglietti, J.: Modeling large-scale inundation of Amazonian seasonally flooded wetlands, Geophys. Res. Lett., 34, L15404, doi:10.1029/2007GL030156, 2007.

Wood, A. W., Maurer, E., Kumar, A., and Lettenmaier, D. P.: Long-range experimental hydrologic forecasting for the eastern United States, J. Geophys. Res., 107, 4429, doi:10.1029/2001JD000659, 2002.

Yamazaki, D., Kanae, S., Kim, H., and Oki, T.: A physically n dynamics in a global river routing model, Water Resour. Res., 47, W04501, doi:10.1029/2010WR009726, 2011.

Discussion Paper | Discussion Paper | Discussion Paper | Discussion Paper |

Table 1. Summary of the performance of *in situ* discharge data assimilation (Exp 1): median Nash and Suttcliffe index (E_{NS}) in simulation (Open-loop) and assimilation (EnKF) modes and mean change in root mean square error (Δrms).

Sites		Exp. 1a[b] E_{NS}	Exp. 1a[b] Δrms (%)	Exp. 1b[c] E_{NS}	Exp. 1b[c] Δrms (%)	Exp. 1c[d] E_{NS}	Exp. 1c[d] Δrms (%)
All	Open-loop	0.68	–	0.68	–	0.68	–
	EnKF	0.93	−42	0.72	−8	0.85	−25
Assimilation	Open-loop	0.71	–	0.89	–	0.71	–
	EnKF	0.94	−49	0.98	−51	0.88	−29
Validation	Open-loop	0.60	–	0.65	–	0.60	–
	EnKF	0.73	−16	0.67	−3	0.67	−10
Large rivers[a]	Open-loop	0.79	–	0.79	–	0.79	–
	EnKF	0.94	−34	0.87	−23	0.95	−40

[a] Stream gauges located at rivers reaches with upstream drainage area larger than 10^5 km^2.
[b] Exp. 1a – data assimilation using discharge from 80 % of the stream gauges.
[c] Exp. 1b – data assimilation using discharge from 10 % of the stream gauges.
[d] Exp. 1c – equal Exp. 1a but without transforming discharge into the log space.

Table 2. As Table 1 but for Exp. 2.

	Sites		E_{NS}	Δrms (%)
All	Radar altimetry	Open-loop	0.66	–
	Assimilation	EnKF	0.96	−56.0
	In situ stage	Open-loop	0.64	–
	Validation	EnKF	0.74	−13
	In situ discharge	Open-loop	0.68	–
	Validation	EnKF	0.68	1
Inside	In situ stage	Open-loop	0.75	–
ENVISAT	Validation	EnKF	0.94	−44
domain*	In situ discharge	Open-loop	0.79	–
	Validation	EnKF	0.86	−15

* Upstream and downstream at least one altimetry station.

Discussion Paper | Discussion Paper | Discussion Paper | Discussion Paper |

Table 3. As Table 1 but for Exp. 3.

	Sites		E_{NS}	Δrms (%)
All	Altimetry discharge	Open-loop	0.62	–
	Assimilation	EnKF	0.79	−23
	In situ discharge	Open-loop	0.68	–
	Validation	EnKF	0.72	−5
Inside ENVISAT Domain*	In situ discharge	Open-loop	0.76	–
	Validation	EnKF	0.80	−15

* Upstream and downstream at least one altimetry station.

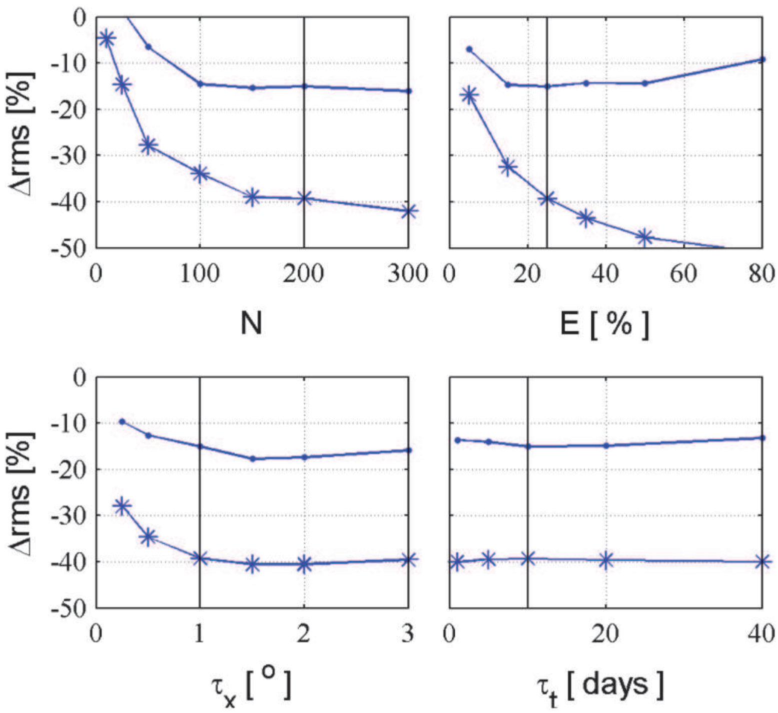

Fig. 1. Sensitivity tests of DA scheme parameters. Mean change in root mean square error (Δrms) for the assimilation (line with stars) and validation (line with dots) stream gauges as function of ensemble size (N), precipitation relative error (E) and spatial (τ_x) and temporal (τ_t) decorrelation lengths of precipitation errors. First guess values are represented by the black line.

Discussion Paper | Discussion Paper | Discussion Paper | Discussion Paper |

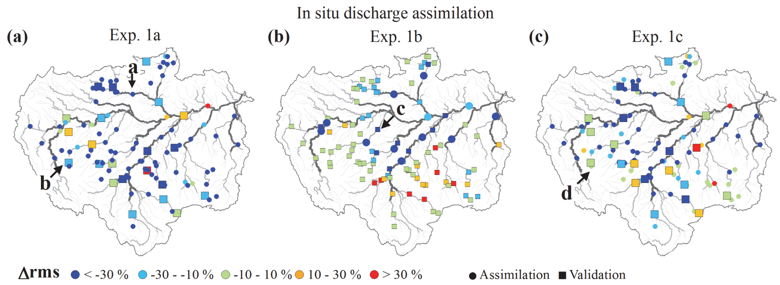

Fig. 2. Evaluation of in situ discharge assimilation. Spatial distribution of change in root mean square error (Δrms) in stream gauges used for data assimilation (circles) and validation (squares) considering the assimilation of **(a)** almost all gauges (Exp. 1a), **(b)** only 12 gauges (Exp. 1b) and **(c)** almost all gauges but without log transformation (Exp. 1c).

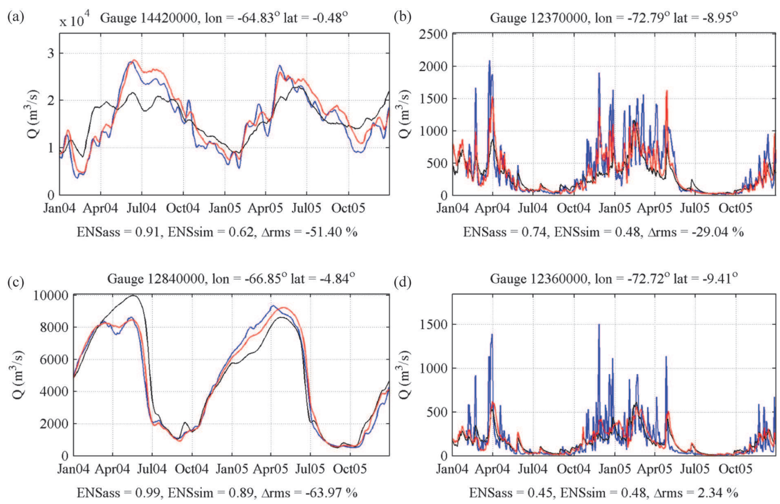

Fig. 3. Discharge derived from in situ observation (blue line), open-loop simulation (black line) and EnKF simulation (red line) at **(a)** Negro River (assimilation site, Exp. 1a), **(b)** upper Juruá River (validation site, Exp. 1a), **(c)** lower Juruá River (validation site Exp. 1b) and upper Juruá River (assimilation site, Exp. 1c). Site are indicated Fig. 2.

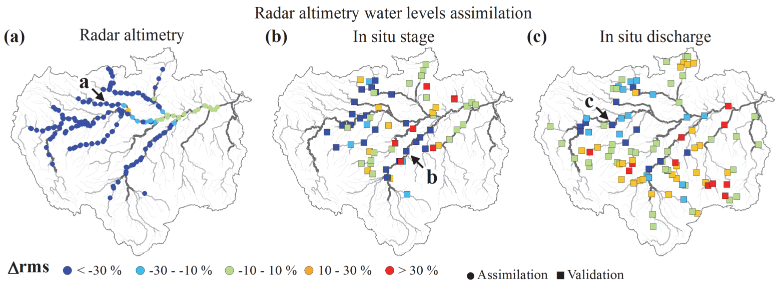

Fig. 4. Evaluation of ENVISAT radar altimetry data assimilation. Spatial distribution of change in root mean square error (Δrms) at **(a)** altimetry stations used for data assimilation and stream gauges with **(b)** stage and **(c)** discharge data used for verification.

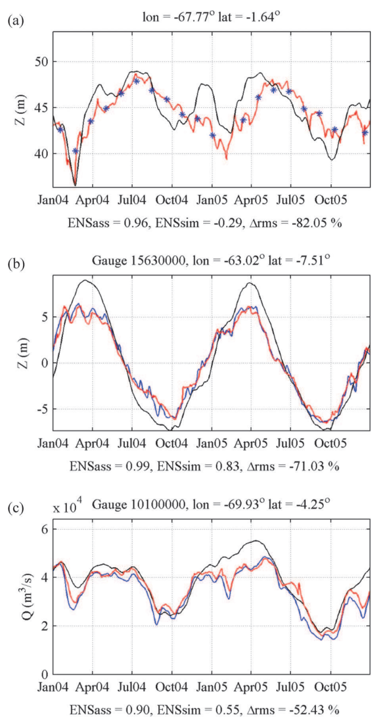

Fig. 5. Observation (blue line), open-loop simulation (black line) and EnKF simulation (red line) at **(a)** Japurá River altimetry site, **(b)** Madeira River in situ stage site **(c)** Solimões River in situ discharge site. Sites are indicated in Fig. 4.

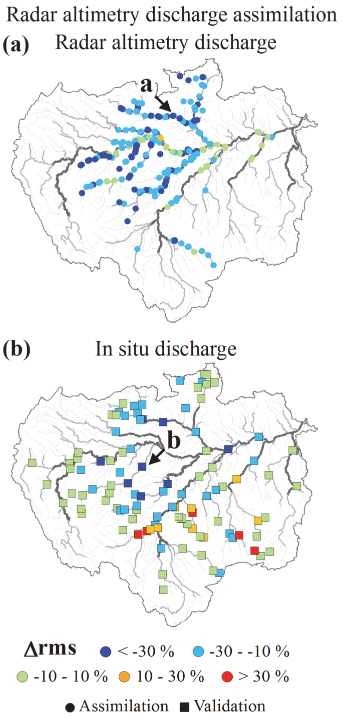

Fig. 6. Evaluation of ENVISAT radar altimetry discharge assimilation. Spatial distribution of change in root mean square error (Δrms) at **(a)** altimetry stations used for data assimilation and **(b)** stream gauges with discharge data used for validation.

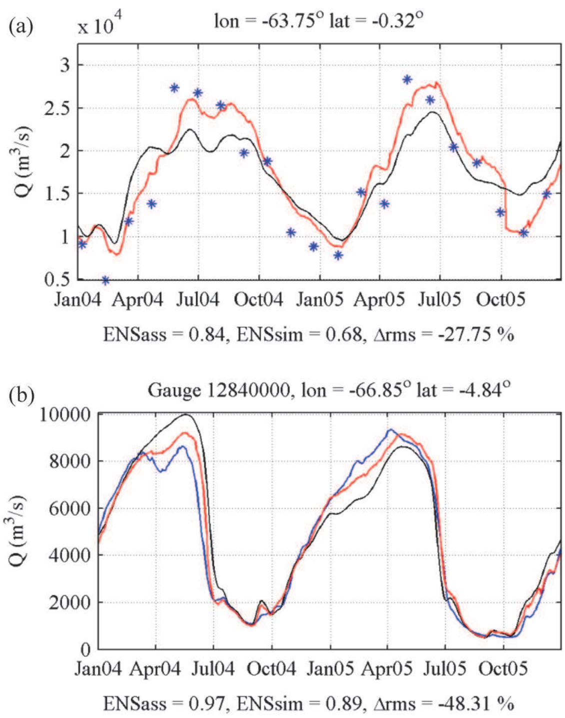

Fig. 7. Observation (blue line), open-loop simulation (black line) and EnKF simulation (red line) of discharge at **(a)** Negro River altimetry site and **(b)** Juruá River in situ site. Sites are indicated in Fig. 6.

Discussion Paper | Discussion Paper | Discussion Paper | Discussion Paper |

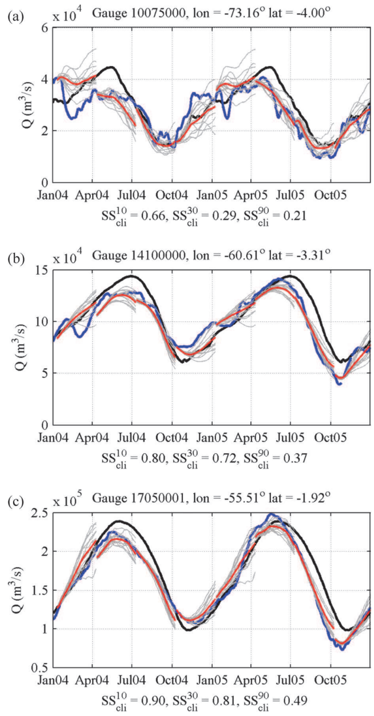

Fig. 8. Evaluation of streamflow forecasts. Observed (blue), climatological (black) discharges, ensemble forecasts (grey) together with ensemble mean (red) at **(a)** Upper Solimões River at Tamishiyacu, **(b)** Solimões River at Manacapuru and **(c)** Amazon river at Óbidos. Presented forecasts started each 10 January, April, July and October. Sites are indicated in Fig. 9.

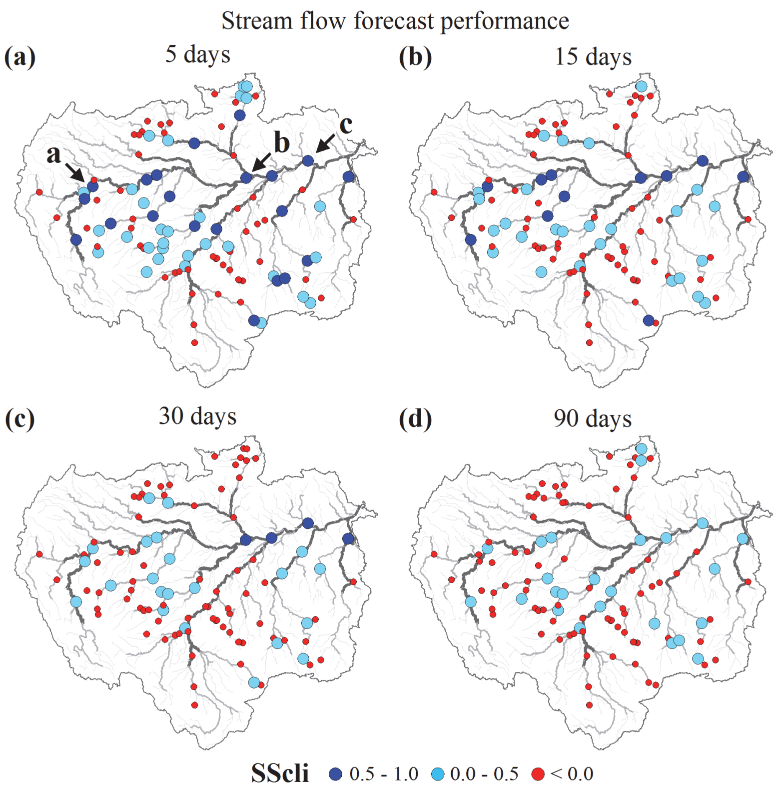

Fig. 9. Evaluation of streamflow forecasts. Spatial distribution of the skill score SS_{cli} for **(a)** 5, **(b)** 15, **(c)** 30 and **(d)** 90 days lead time.

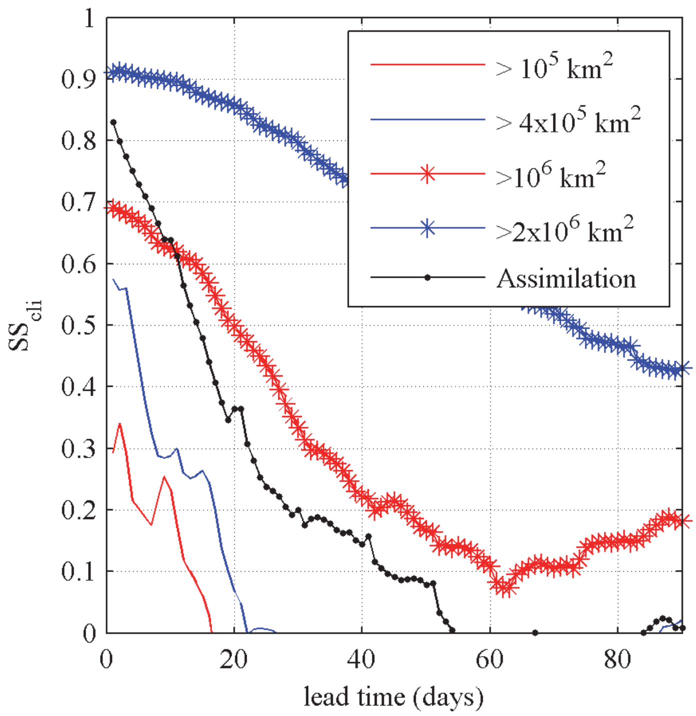

Fig. 10. Median skill score SS_{cli} of stream flow forecasts at gauging stations as function of lead time. Different curves show results considering gauges with different drainage areas (red and blue lines) and only gauges used for data assimilation (black line with dots).